A. de Rooij

Materials and Processes Division, ESTEC, Noordwijk, The Netherlands

Bimetallic Compatible Couples

Abstract

In the construction of a satellite, two metals that form a compatible couple may have to be placed in close proximity to one another. Although this may not cause anomalies or malfunctions in the space environment, it has to be borne in mind that spacecraft often have to be stored on earth for considerable periods of time and that during storage they may inadvertently be exposed to environments where galvanic corrosion can take place. In fact, this is known to have taken place on several occasions and it is for this reason that the Agency has been studying the dangers involved.

The static corrosion potential for a large number of metals and alloys has been established. These potentials were measured in a 3.5 % NaCl solution representing a standard corroding atmosphere. The potentials measured have been compared against the data for similar materials to be found in the literature. Data for material combinations not tested in the present study have been compiled from the literature in order to make available one complete reference table.

It is shown that, in the case of atmospheric galvanic corrosion, a simplified procedure can be used to estimate the compatibility of a bimetallic couple by taking into account the difference between the two static potentials of the materials involved.

1. Introduction

This paper is concerned with the reactions occurring when two dissimilar metals are in direct electrical contact in corrosive solutions or atmospheres. The driving force for the galvanic corrosion experienced is the difference in electrode potential between the two dissimilar metals, where the less resistant metal becomes the anode and the more resistant the cathode. Under these conditions the cathodic metal (the more positive component of the bimetallic couple) corrodes very little or not at all, while the corrosion of the anodic metal (the more negative member of the bimetallic couple) is greatly enhanced with respect to the uncoupled corrosion rate in the same environment.

In general, the potential difference between the metals forming the bimetallic couple is not a decisive factor in the corrosion of the anodic member, and it is often stated that no generally valid galvanic formula for corrosion under atmospheric conditions can be constructed.

These problems have been studied extensively in a number of investigations and large test programmes have been set up to examine the corrosion behaviour of bimetallic couples under different atmospheric conditions. [1,2] A comprehensive set of tables giving the additional corrosion of bimetallic couples of metals and alloys under atmospheric and immersed conditions is published by the British Standards Institution. [3]

Some of these investigations have been carried out over periods of 22 years of exposure. A comprehensive bibliography can be found in Reference 4.

The main limitation of these investigations in relation to space hardware lies in the assessment of the amount of corrosion that is acceptable. A metal stated to exhibit 'very slight additional corrosion, usually tolerable in service,' is often not acceptable for space hardware.

2. General theory

2.1 Galvanic corrosion

One of the basic differences between electrochemical corrosion and that due to a purely chemical action is that the overall chemical reaction of a reagent with a metal in electrochemical corrosion is divided into two largely independent processes:

- transfer of metal into the solution with an equivalent number of electrons left in the metal, called the anodic process, and
- assimilation of the excess electrons in the metal, called the cathodic process.

Electrochemical corrosion is, in principle, characterised by localisation of the anodic and cathodic processes in different regions. These different regions can be found on the same metal surface between different microscopic phases, as well as between two dissimilar metals electrically in contact with each other. The direction of the electrochemical process between two dissimilar metals or phases depends on the difference between the two Gibbs free energies (ΔG). A large negative value of $\Delta(\Delta G)$ indicates a pronounced tendency for the corrosion couple to react with its environment.

The tendency for a bimetallic couple to corrode can also be expressed in terms of the electromotive force (EMF) or the static corrosion potential of the corrosion cell. The relation between AG and EMF is defined by:

$$\Delta(\Delta G) = -AE.n.F \qquad (1)$$

where

n = number of electrons taking part in the reaction
ΔE = EMF (difference between the EMFs of the two members of the corrosion couple
F = Faraday's constant.

Tendency to corrode is not a measure of the corrosion rate. A large negative value of ΔE may or may not be accompanied by a high corrosion rate.

The principal phases in the operation of a galvanic corrosion cell are illustrated in

Figure 1. The less noble metal acts as the anode and is oxidised according to:

$$Me \leftrightarrow Me^{n+} + ne^- \quad (2)$$

The cathodic process in atmospheric corrosion is often stated in terms of the oxygen reduction (ionisation of oxygen):

$$O_2 + 2H_2O + 4e \leftrightarrow 4OH^- \quad (3)$$

Current flow between anodes and cathodes will take place in the metal by the movement of electrons from anodic to cathodic regions and in the solution by movement of cations from the anodic to the cathodic regions and movement of anions in the opposite direction. The material effect of metal corrosion will therefore appear principally on the anodes. On the cathodic areas there will be no appreciable loss of metal.

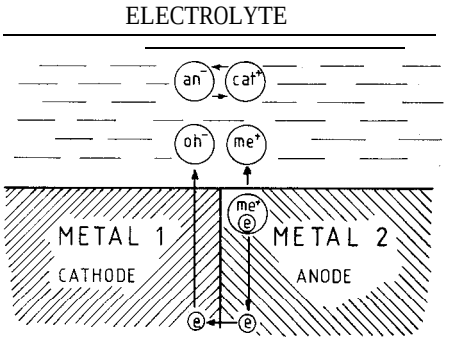

Figure 1. Galvanic corrosion cell:
(1) the cathodic process, which is the acceptance of electrons by an atom or ion capable of being reduced on the cathode;
(2) the anodic process, which is the transfer of metal ions into the solution

2.2 Bimetallic corrosion in atmospheres

The electrolyte in atmospheric environments consists of a thin condensed film of moisture containing any soluble contaminants in the atmosphere such as acid fumes, chlorides etc. The formation of this film depends mainly on three important variables: temperature, relative humidity and the presence of dust particles in the atmosphere.

The characteristics of a moisture film on a surface are not necessarily the same as those of a bulk electrolyte. In a moisture film, the replenishment of dissolved oxygen is much greater than in bulk electrolyte, owing to the large ratio of surface area to electrolyte volume. Under conditions of lowered relative humidity, which permits rapid evaporation, convective mixing in the condensed layer further hastens the arrival of dissolved oxygen at the cathode. Both characteristics of the moisture film can result in an increase in galvanic corrosion rate.

Secondly, the electrolyte conductivity of the condensed layer parallel to the surface of the metal is low compared with that of the bulk electrolyte, even when it contains acid fumes or chlorides. This high electrolytic resistance of the thin condensed electrolytic layer has a controlling effect on the distribution of the corrosion. The galvanic attack will normally be highly localised and is rarely found much further than 25 mm from the bimetallic junction.[5] The geometrical anode/cathode area ratio, which for a galvanic couple is an important factor in the observed corrosion rate, is of limited influence. The controlling effect of the electrolytic resistance is equally applicable to anode and cathode of the bimetallic couple. In general, it can be stated that in atmospheric bimetallic corrosion the active areas are small and approximately equal, regardless of the geometrical area ratios.

2.3 Condensation of moisture on surfaces

A thin condensed film of moisture can be formed on surfaces at a relative humidity of less than 100%, i.e. at a temperature above the dew point. The presence of irregularities or flaws on surfaces promotes capillary condensation of moisture under atmospheric conditions. Clearances between contacting surfaces of a structure or the mating parts of an electrical connection, dust on a surface and pores in an already existing oxide film can all form fine capillaries, permitting the condensation of moisture.

Another condensation mechanism is the attraction between water molecules and a solid surface. This formation of an extremely thin layer of condensed water molecules bound to the surface by absorption forces is called ‘absorption condensation’ and can take place at a relative humidity of less than 100%.

A further increase in the thickness of the condensed moisture layer is brought about by chemical reactions between the adsorbed layer and the material on which condensation occurs (Fig. 2). The formation of hydrated compounds enhances the condensation, because of the lowered water vapour pressure above the crystal hydrates.

It is clear from the above that the possibility of moisture condensation has to be considered even when relative humidities are lower than 100%. However, this

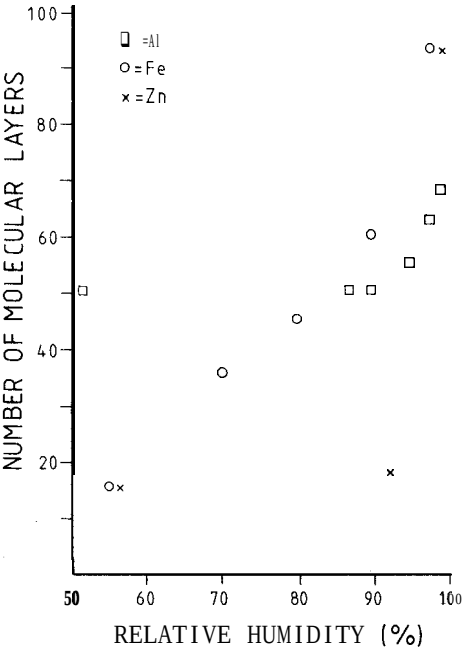

Figure 2. Relationship of relative humidity to the thickness of an adsorbed film of moisture on a clean, finely polished iron surface[6,7,8]

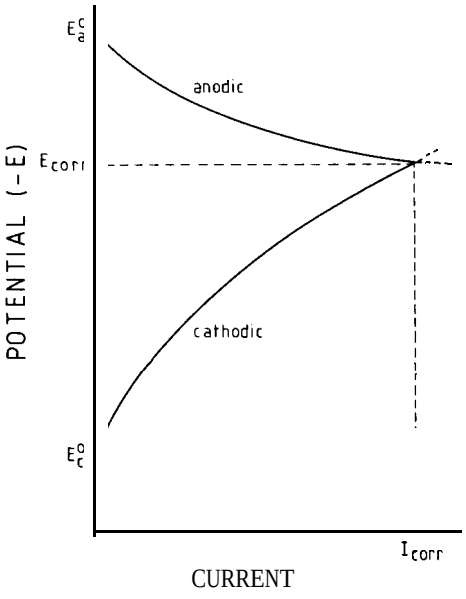

Figure 3. Anodic and cathodic polarisation curve of a bimetallic couple

condensation depends not only on the moisture content, but also on the presence of gaseous impurities in the air, corrosion products or other films that might be present on the surface and surface irregularities.

2.4 **Anodic and cathodic behaviour of couples**

If two electrodes of different potential are immersed in an electrolyte, a potential difference exists given by the difference between the initial static potentials. If the two electrodes are electrically connected, this difference will diminish to a compromise potential, producing the corrosion current. This decrease in the initial potential difference between the electrodes of a galvanic cell is called 'polarisation'. A distinction is made between anodic polarisation (displacement of the anodic potential in the positive direction) and cathodic polarisation (displacement of the cathodic potential in the negative direction). The extent of the electrode activity can be judged by the amount of potential shift. The kinetics of the process can consequently be determined from the relationship between the shift in electrode potential and the current density. This dependence is presented in Figure 3.

Under atmospheric conditions, the anodic polarisation is primarily determined by the 'passivation' of the anode surface as a result of the formation of a continuous oxide film. With the onset of the passive state, the initial anode process is retarded by the passive film formed and the anode potential becomes more positive.

The anode polarisation can be described as:

$$E_A = E_A^{\circ} + R_A \, x \, i \tag{4}$$

where

E_A° = initial anodic potential in the absence of anodic current
i = current
R_A = polarisation resistance of anode (= slope of anode polarisation curve).

The predominant cathodic process, as noted in Section 2.1, is the ionisation of oxygen by which the cathode acts as an oxygen electrode.

The change in cathode potential with current density is subject to the relation:

$$E_C = E_C^{\circ} - n \tag{5}$$

in which n is defined by the Butler-Volmer relation:

$$i/i_o = e^{Kn} - e^{-Kn} \tag{6}$$

where

E_C° = potential of the equilibrium oxygen electrode E_{O2}
i = current
i_o = exchange current density of electrode reaction
n polarisation
K = constant depending on type of cathode reaction.

The limiting current density for the reduction of oxygen is determined by the diffusion coefficient of oxygen in the electrolyte and by the thickness of the electrolyte on the cathode surface under atmospheric conditions. Turbulence in this surface layer, resulting in a higher oxygen concentration, increases the limiting current density of the oxygen reduction. The low current densities under galvanic corrosion under atmospheric conditions and the relatively high limiting current density for oxygen reduction ensure that under the given circumstances the ionisation of oxygen is the predominant cathodic process. A general cathodic polarisation curve is shown in Figure 4.

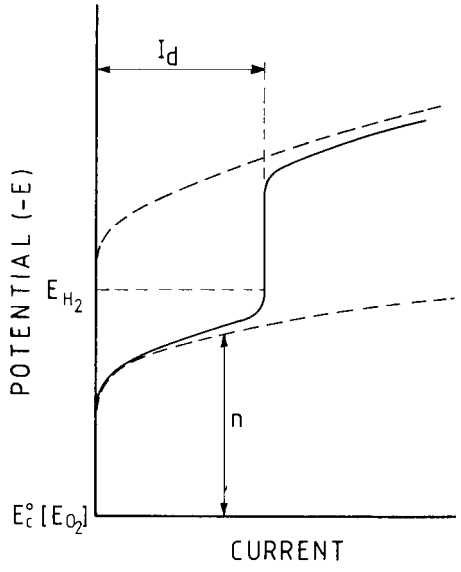

Figure 4. Cathodic polarisation curve, showing oxygen-ionisation overvoltage and the limiting diffusion-current density

3. Materials

Most materials investigated are those commonly in use in the aerospace industry. Besides the usual steels, copper alloys and aluminium alloys, many joining materials, such as solder and braze alloys, have also been examined.

Pure metals such as gold, platinum, silver, copper and nickel are of interest, since they are used for plating other metals and alloys. This plating is performed for various reasons, which range from a need to provide general corrosion protection, through maintenance of stable optical properties, decreasing electrical contact resistance and increasing solderability, to specialised RF shielding applications.

Some of the pure metals listed are not permitted for spacecraft use (e.g. tin, cadmium and zinc), while others such as rhenium, erbium and uranium are unlikely to be selected and are only added for the sake of completeness.

4. Sample preparation

Most of the samples investigated have been collected over a period of several years by the ESTEC Metals Laboratory. They were originally materials submitted for quality investigations or intended as metal and alloy stock. Before these samples were used for the electrochemical tests, they were ground on wet grinding paper nr. 1200 and ultrasonically cleaned in isopropanol. The first attempt to measure the static potentials was undertaken straight after this sample preparation. These measurements were not completely reproducible. Leaving the samples for at least one day in the laboratory atmosphere after grinding improved the reproducibility significantly, and this waiting period was subsequently adopted as a standard procedure for all samples prior to testing.

5. Method of investigation

The corrosion behaviour of an electrolytic cell is determined by the difference in static corrosion potential, the corrosion current and the presence of an electrolyte. The corrosion rate depends on the corrosion current and is a function of the geometrical area ratio, the resistance of the electrolyte, and the materials in the cell. As already noted in Section 2, the geometrical area ratio between anode and cathode is of lesser importance in bimetallic electrolyte corrosion, while the electrolyte usually consists of condensed vapour containing some acid fumes and chlorides. This environment is simulated by means of a 3.5 % NaCl water solution representing the composition of human perspiration and/or industrial/marine atmospheres. No special device has been designed for simulating moisture films on surfaces; instead, to simulate the rapid convective mixing and the replenishment of dissolved oxygen, the electrolyte is agitated by magnetic stirring.

A 100 ml glass beaker filled with the electrolyte solution is placed on a hotplate. The temperature of the electrolyte is stabilised slightly above room temperature to ensure a constant temperature. Two electrodes, one being the reference electrode (saturated calomel electrode), the other the metal or alloy to be investigated, are connected to a high-impedance digital voltmeter (DVM). While the real EMF of an electrolytic cell is being measured, no current flow is allowed between the two electrodes. The experimental setup is illustrated in Figure 5.

The EMF between the two electrodes is recorded as a function of time on a graphical recorder connected to the DVM. After a certain length of time, the EMF stabilises to a constant value. Owing to the sample preparation procedure, 'passivation' layers (oxide layer) are present on the sample surface. These surface layers are normally found on electronic and engineering materials exposed to atmospheric conditions. In order to ensure that measurements are made on an active electrode surface, the sample surface can be ground during the measurements in the electrolyte solution or the stirring can be stopped to reduce the oxygen concentration in the electrolyte and let the chloride ions break down the 'passivation' layer. Both types of test have been performed, but in most cases the results were not very reliable. The results for active electrodes are taken from the literature.[6,9-12,14]

The distance between the electrodes and their size is of minor importance when the EMF of an electrolytic cell is being measured; only the current is influenced by these parameters.

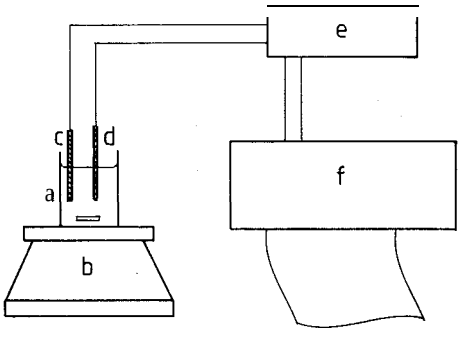

Figure 5. Experimental setup
(a) 100 ml beaker containing electrolyte
(b) botplate with magnetic stirrer
(c) reference electrode
(d) sample
(e) digital voltmeter
(f) recorder

Table 1. Electromotive force of metals and alloys measured in 3.5% NaCl with respect to a calomel electrode

EMF vs. calomel electrode (V)	Material	EMF vs. calomel electrode (V)	Material
+0.17	Platinum	-0.27	CDA 521 (7Sn,rem Cu)
+0.15	Carbon	-0.27	CuAl10Fe (10Al,3Fe,rem Cu)
+0.15	Gold	(−0.28)[6]	Inconel 92 (71Ni,16Cr;,7Fe,3Ti,2Mn) active
+0.08	Rhenium	-0.29	CuA112 (12Al,rem Cu)
+0.04	Tantalum	(−0.30)[13]	Niobium (1Zr,rem Nb)
-0.03	Silver	-0.30	Tungsten
(---)[14]	AM350 (17Cr,4.2Ni,2.7Mo) passive	(−0.30)[6]	Nickel active
-0.07	A286 (15Cr,25Ni,Mo,Ti,V) passive	(−0.31)[6]	Chromium active
(—)[14]	AM355 (15.5Cr,4.3Ni,2.7Mo) passive	(−0.32)[13]	Cobalt
(—)[14]	Carpenter 20 (20Cr,28.5Ni,2.25Mo,3.25Cu) passive	-0.33	Nitrinol (45Ti,55Ni)
(—)[14]	AISI 201 (8.7Mn,18Cr,5Ni) passive	-0.38	Invar (36Ni,rem Fe)
-0.07	AISI 316 (18Cr,13Ni,2Mo,rem Fe) passive	-0.39	Cerrotric (42Sn,rem Bi)
-0.08	AISI 321 (18Cr,10Ni,0.4Ti) passive	-0.42	SnAg4C3.5 solder
-0.08	AISI 347 (18Cr,12Ni, +Nb,rem Fe) passive	-0.43	Sn95Ag4.9In0.1 solder
-0.09	AISI 301 (17Cr,7Ni) passive	-0.46	SnAg4 solder
-0.10	AISI 304 (19Cr,10Ni,rem Fe) passive	-0.46	SnAg5 solder
-0.10	Hastelloy C (17Mo,15Cr,5W,6Fe,rem Ni) passive	-0.46	Tin
-0.10	Nichrome (80Ni,20Cr) passive	-0.48	Sn10Sb solder
-0.10	Monel 60 (65Ni,0.2Fe,3.5Mn,2Ti,27Cu)	-0.48	Indalloy no. 10 (75Pb,25In) solder
-0.11	Inconel 92 (71Ni,16Cr,7Fe,3Ti,2Mn) passive	-0.49	Indalloy no.7 (50Pb,50In) solder
(—)[14]	CDA 655 (3.5Si,rem Cu)	(−0.49)[9]	AISI 316 (18Cr,13Ni,2Mo,rem Fe) active
-0.11	17-7 PH stainless st. (17Cr,7Ni,1.1Al) passive	-0.50	Lead
-0.11	AISI 309 (23Cr,13Ni) passive	(−0.51)[14]	AISI 347 (18Cr,12NI,+Nb,rem Fe) active
-0.12	Titanium	-0.51	Sn63 (63Sn,37Pb) solder
-0.12	Monel 400 (32Cu,2.5Fe,2Mn,rem Ni)	-0.51	Sn60 (60Sn,40Pb) solder
-0.12	CDA 442 (71Cu,1Sn,38Zn)	-0.51	Sn62Ag2 (62Sn,36Pb,2Ag) solder
-0.12	CDA 715 (70Cu,30Ni)	-0.51	Sn59Sb2 (59Sn,39Pb,2Sb) solder
-0.12	Molybdenum	-0.51	Sn60Sb5 (60Sn,35Pb,5Sb) solder
-0.16	CDA 510 (96Cu,4Sn,P) phosphor bronze	-0.51	Sn60Sb10 (60Sn,30Pb,10Sb) solder
-0.17	AISI 420 (0.35C,13Cr,rem Fe) passive	-0.51	Sn60Pb39.5 (Cu0.12,P0.9) solder
-0.17	AISI 434 (0.12C,17Cr,1Mo,rem Fe) passive	-0.51	PbSn5Ag1.5 solder
-0.17	Bismuth	-0.52	Mild steel
-0.18	Nickel passive	(−0.53)[14]	AISI 304 (19Cr,10Ni,rem Fe) active
-0.18	Monel 67 (67.5Cu,31Ni,0.3Ti,0.5Fe)	(−0.56)[14]	AISI 420 (0.35C,13Cr,rem Fe) active
-0.18	Copper Phosphorous (4.5P,rem Cu)	(−0.56)[14]	AISI 434 (0.12C,17Cr,1Mo,rem Fe) active
-0.19	Copper Phosphorous (8.5P,rem Cu)	-0.56	AA 2219-T3,T4 (6.3Cu,0.3Mn,0.18Zr,0.1V,0.06Ti,rem Al)
-0.20	Copper Phosphorous (10.5P,rem Cu)	(−0.59)[6]	AISI 440B (17Cr,0.5Mo,rem Fe) active
-0.20	Copper	-0.61	AA 2014-T4 (4.5Cu,1Fe,1Si,0.15Ti,rem Al)
-0.20	CDA 110 (electrolytic tough pitch)	-0.61	AA 2017-T4 (4Cu,1Fe,1Mg,0.1Cr,rem Al)
-0.20	CDA 172 (2Be,rem Cu)	-0.62	AA 2024-T3,T4 (4.5Cu,1.5Mg,0.6Mn,rem Al)
-0.20	Gold-Germanium solder (12Ge,rem Au)	(−0.63)[13]	AA B295.0-T6 (2.5Si,1.2Fe,4.5Cu,rem Al) casting
-0.20	Copper-Gold (25Au,rem Cu)	(−0.64)[13]	AA 295.0-T6 (1Si,1Fe,4.5Cu,rem Al) casting
-0.23	AISI 440B (17Cr,0.5Mo,rem Fe) passive	-0.64	In75Pb25 solder
(—)[14]	Titanium 13V,11Cr,3Al	-0.65	Indalloy no. 1 (50In,50Sn) solder
(---)[14]	Titanium 8Mn	(−0.66)[13]	AA 380.0-F (8.5Si,2Fe,3.5Cu,rem Al) casting
(---)[14]	Titanium 5Al,2.5Sn	(−0.66)[13]	AA 319.0-F (6Si,1Fe,3.5Cu,rem Al) casting
-0.24	Ti6Al4V (6Al,4V,rem Ti)	(−0.66)[13]	AA 333.0-F (9Si,1Fe,3.5Cu,rem Al) casting
-0.24	Silicon	-0.67	Indium
-0.25	CDA 240 (80Cu,20Zn)	(−0.68)[13]	AA 208.0-F (3Si,1.2Fe,4Cu,rem Al) casting
-0.25	CDA 220 (90Cu,10Zn)	(-0.69)[13]	AA 850.0-T4 (0.7Si,0.7Fe,1Cu,1Ni,rem Al) casting
-0.25	CDA 752 (65Cu,18Ni, 17Zn)	-0.69	AA 2014-T6 (4.5Cu,1Fe,1Si,0.15Ti,rem Al)
-0.26	CDA 280 (60Cu,40Zn)	-0.70	Cadmium
-0.26	CDA 464 (60Cu,1Sn,39Zn)	(−0.71)[13]	AA 355.0-T6 (5Si,0.6Fe,1.3Cu,rem Al) casting
(—)[14]	Uranium 8Mo	-0.71	AA 2024-T81 (4.5Cu,1.5Mg,0.6Mn,rem Al)
-0.26	CDA 270 (63Cu,37Zn)	-0.72	AA 2219-T6,T8 (6.3Cu,0.3Mn,0.18Zr,0.1V,0.06Ti,rem Al)
-0.27	CDA 298 (52Cu,48Zn)	-0.72	AA 6061-T4 (1Mg,0.6Si,0.25Cu,0.2Cr,rem Al)
(−0.27)[6]	Nichrome 80/20 (80Ni,20Cr) active	(−0.73)[13]	AA 413.0 (12Si,2Fe,1Cu,rem Al) casting

Table 1. Electromotive force of metals and alloys measured in 3.5% NaCl with respect to a calomel electrode (continued)

EMF vs. calomel electrode (V)	Material	EMF vs. calomel electrode (V)	Material
(−0.73)[13]	AA B443.0 (5Si,0.8Fe,rem Al) casting	-0.77	AA 5086 (4Mg,0.5Mn,rem Al)
(−0.73)[13]	AA 356.0-T6 (7Si,0.6Fe,rem Al) casting	-0.78	AA 5154 (3.5Mg,0.25Cr,rem Al)
(−0.73)[13]	AA 360.0 (9.5Si,2Fe,0.6Cu,rem Al) casting	-0.78	AA 5454 (2.8Mg,1Mn,0.2Ti,0.1Cu,0.2Cr,rem Al)
-0.74	AA 4043 (12Si,1Cu,1Mg,rem Al)	-0.78	AA 4047 (12Si,rem Al)
-0.74	AA 6151 (1Mg,1Fe,0.25Zn,0.15Ti,rem Al)	-0.78	Al-C
-0.74	AA 7075-T6 (5.6Zn,2.5Mg,1.6Cu,0.3Cr,rem Al)	(−0.78)[13]	Uranium
-0.74	AA 7178-T6 (6.8Zn,3Mg,2Cu,0.2Ti,rem Al)	-0.79	AA 5056 (5.2Mg,0.1Mn,0.1Cr,rem Al)
-0.75	AA 1160 (98.4Al)	(−0.79)[13]	AA 7079-T6 (4.3Zn,3.3Mg,0.6Cu,0.2Mn,0.2Cr,rem Al)
-0.75	Aluminium	-0.79	AA 5456 (5Mg,0.7Mn,0.15Cu,0.15Cr,rem Al)
-0.75	AA 5356 (5Zn,0.1Ti,0.1Cr,rem Al)	-0.79	AA 5083 (4.5Mg,0.7Mn,rem Al)
-0.75	AA 5554 (5Mg,1Mn,0.25Zn,0.2Cr,rem Al)	(−0.79)[13]	AA 514 (4Mg,rem Al) casting
-0.75	AA 1050 (99.5Al)	(−0.79)[13]	AA 518 (8Mg,0.8Fe,0.05Ni,0.05Sn,rem Al) casting
-0.75	Al-3Li	(−0.84)[13]	AA 520.0-T4 (10Mg,0.2Cu,0.2Ti,rem Al) casting
-0.75	AA 1100 (99.0Al)	(−0.85)[13]	X7005-T6,T63 (4.8Zn,1.5Mg,0.2Cr,rem Al)
-0.75	AA 3003 (1.2Mn,rem Al)	(−0.85)[13]	AA 7039-T6,T63 (4Zn,3Mg,0.2Cr,rem Al)
-0.75	AA 6151 (1Mg,1Fe,0.8Mn,0.25Zn,0.15Ti,rem Al)	-0.87	AA 7072 (1Zn,0.5Si,0.3Cr,rem Al)
-0.75	AA 6053 (1.3Mg,0.5Si,0.35Cr,rem Al)	(−0.90)[13]	AA A712 (6.5Zn,0.8Mg,rem Al) casting
-0.75	AA 6061-T6 (1Mg,0.6Si,0.25Cu,0.2Cr,rem Al)	-0.97	Beryllium
-0.75	AA 6063 (0.7Mg,0.4Si,rem Al)	-1.03	Zinc
-0.75	Alclad 2014 (4.5Cu,1Fe,1Si,0.15Ti,rem Al)	-1.21	Manganese
-0.75	Alclad 2024 (4.5Cu,1.5Mg,0.1Cr,rem Al,Al-clad)	-1.34	Erbium
-0.76	AA 3004 (1.5Mn,1Mg,rem Al)	-1.55	Electron (4Zn, 0.7Zr, rem Mg)
-0.76	AA 1060 (99.6Al)	-1.57	ZW3 (3Zn, 0.5Zr, rem Mg)
-0.76	AA 5050 (1.5Mg,rem Al)	-1.58	AZ61 (6Al,1Zn,0.3Mn,rem Mg)
-0.76	AA 7075-T73 (5.6Zn,2.5Mg,1.6Cu,0.3Cr,rem Al)	-1.60	AZ31B (3Al,1Zn,rem Mg)
-0.77	AA 5052 (2.5Mg,0.25Cr,rem Al)	-1.60	Magnesium

6. Results

The values compiled in Table 1 are a combination of the results of the tests described in Sections 4 and 5 and data from the published literature (see reference list).

The EMF is given in volts relative to a saturated calomel electrode. In some published reports, [6] the potential is given relative to the standard hydrogen electrode. The potential difference between this electrode and the saturated calomel electrode used here is -0.2416 V at room temperature. To derive the potential relative to the standard hydrogen electrode, therefore, 0.2146 V has to be added to the values displayed in Table 1. The EMFs for the metals examined are given in descending order, with the noble materials at the top.

The results for metals and alloys taken from the literature are referenced. Other metal and alloy data found in the literature and also those measured during our tests have been carefully scrutinised to determine whether the same environment and reference electrode have been used. In some references, no values for the static corrosion potential are given, but only the position in the galvanic series. If an unmeasured material is taken from these series, a careful interpolation has been performed with the aid of known potentials of nearby materials.

7. Discussion

7.1 General aspects

As explained in Section 2.4, the two electrode processes involved in the galvanic action are an anodic process on the metal with the lower static potential, and an oxygen reduction process on the metal with the higher static potential. This means that the initial potential difference is not given by the difference in initial static potentials of the metals involved in the reaction, but by the difference between the initial static

potential of the anode material and the initial potential of the oxygen reaction on the cathode material.

To enable the extent of the corrosion at the anode under atmospheric circumstances to be determined, the corrosion current of the galvanic corrosion cell has to be established under the same conditions. In the literature, however, there is a notable lack of quantitative data on the kinetics of the electrochemical processes that take place on the surface of a metal under absorbed moisture films. Limited quantitative data on anodic polarisation at different humidity levels is to be found in Russian literature. [6] These data are given in Table 2.

Table 2. Dependence of anodic polarisation of metals on the atmospheric humidity (Ref. 6)

Relative humidity (%)	Anodic polarisation (V/A) Al	Zn	Fe
50	—	10^7	—
75	7×10^4	2×10^5	1×10^5
100	8×10^3	11×10^3	10×10^3

The anodic polarisation is found to be very high initially and gradually to increase with time. The anodic polarisation increases at a particularly high rate as the relative atmospheric humidity decreases. This strong effect can be explained by 'passivation' of the anode surface as a result of the formation of a continuous oxide film. The thinner the moisture film on the electrode surface (i.e. the lower the humidity), the higher the concentration of oxygen is in the electrolyte, resulting in faster formation of the 'passivation' layer on the anode's surface.

Moreover, owing to the unhindered transport of oxygen to the cathode, the speed of the cathodic oxygen-reduction process increases, resulting in a reduced polarisation of the cathode, as opposed to a stagnant electrolyte solution. Once past the initial change in potential, where the electrode potential changes dramatically within a few microamps, the cathode polarisation levels out to an almost constant value depending on the cathode material. Experimental values for the oxygen ionisation overvoltage for various metals can be found in several textbooks on galvanic corrosion. For consistency, the experimental curves are taken from the same reference[6] and are displayed in Figure 6.

The ionisation overvoltage is described by Equations 5 and 6. For high overvoltages, Equation 6 reduces to a single exponential equation, and when the logarithm is taken from both sides, the well-known Tafel equation appears:

$$n = a + b \times \log i \tag{7}$$

where

n = overvoltage
a = $-\log (i_o)/K$
b = $2.303/K$.

For very low overvoltage values, Equation 6 reduces to a linear equation. Using the approximation $e^x \rightarrow 1 + x$ for $x \rightarrow 0$, we can write:

$$n = i/(2 X K) \tag{8}$$

Combining the anodic polarisation curves with the cathodic ones provides information about the corrosion current of the operating cell. The amount of corrosion of the anode is proportional to the corrosion current I:

$$Q = k.Z \tag{9}$$

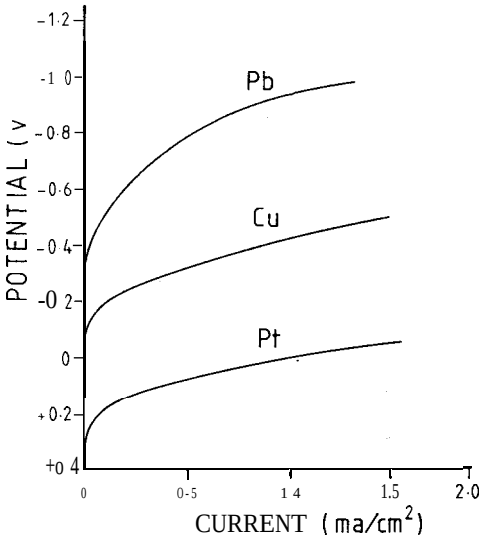

Figure 6. Experimental oxygen-ionisation overvoltage curves for various metals

where

Q = amount of corrosion
I = corrosion current in amperes

$$k = \frac{t.M}{F.n}$$

t = time of current passage in seconds
M = atomic weight of the metal
F = Faraday's constant
n = valence of the metal.

The corrosion current is calculated with the aid of the anodic polarisation data of zinc, aluminium and iron given in Table 2 and their static corrosion potentials, and Equations 5 and 6 for the description of the oxygen ionisation overvoltage. The values for the exchange current density and the constant *Kin* Equation 6 are found by fitting the experimental oxygen ionisation overvoltage curves from Figure 7 to Equations 5 and 6. The potential of the oxygen electrode is taken as E_{O2} = 0.16 V. The results of this calculation can be found in Table 3.

Table 3. Corrosion current in $\mu A/cm^2$ and corrosion rate in $mg/dm^2/day$ (between brackets) as a function of relative humidity for several bimetallic couples

Humidity	50%	75%	100%
Au-Zn	0.159(0.46)	6.64(19.4)	93.6(274)
Cu-Zn	0.13 (0.38)	5.04(14.7)	70.9(274)
Pb-Zn	0.084(0.25)	0.95(2.8)	36.2(106)
Au-Al		13.8 (11.1)	92.9 (75)
Cu-Al		9.6 (7.7)	63.6 (51)
Pb-Al		3.97 (3.2)	20.1 (16)
Au-Fe		7.7 (12.8)	57.0 (95)
Cu-Fe		**5.0 (8.3)**	**33.4 (56)**
Pb-Fe		**1.3 (2.2)**	**4.3 (7.2)**

Anodic polarisation data as a function of humidity and experimental oxygen ionisation overvoltage curves are available for only a few materials. To overcome this lack of experimental data, an approximation for the calculation of the corrosion current is necessary. The major simplification is introduced by linearisation of the cathodic polarisation curves, the cathodic potential being taken as independent of the current and equal to the static corrosion potential of the cathode material. This is approximately valid for relatively high currents (more than 5 $\mu A/cm^2$) and moderate humidity levels. Recalculating the bimetallic couples from Table 2 gives the values listed in Table 4.

Table 4. Corrosion current in A/cm^2 and corrosion rate in $mg/dm^2/day$ (between brackets) as a function of relative humidity for several bimetallic couples using $i = (E_c - E_a)/n$ (n =anodic polarisation)

Humidity	50%	75%	100%
Au-Zn	0.118(0.35)	**5.9 (17.3)**	**107 (313)**
Cu-Zn	0.083(0.24)	4.15(12.1)	75.4(220)
Pb-Zn	0.053(0.16)	**2.65 (7.7)**	48.2(141)
Au-Al		**12.9 (10.4)**	**112.5 (91)**
Cu-Al		**7.6 (6.1)**	**68.8 (55)**
Pb-Al		**3.6 (2.9)**	**31.3 (25)**
Au-Fe		**6.7 (11.2)**	67.0(112)
Cu-Fe		**3.2 (5.3)**	**32.0 (53)**
Pb-Fe		**0.2 (0.3)**	**2.0 (33)**

The very good resemblance between the results in Tables 3 and 4 gives us a tool with which to approximate the corrosion currents of other bimetallic couples. Secondly, if we assume that the anodic polarisation of all materials is equal at a certain humidity level (see Table 2 for Al, Zn and Fe), then the difference in static corrosion potentials of the anode and the cathode might be used as an indication of the amount of corrosion of the anode.

In Table 1 some materials appear in two different states, active as well as passive. The galvanic behaviour of these materials can vary considerably, depending on whether the material is active or passive. A very good example of such a material is stainless steel. In a completely passive state, it will act as a very positive contact material, capable of accelerating the corrosion of copper and copper-base alloys. In the completely active state, it will have little effect as a cathode material, capable only of somewhat increasing the corrosion of aluminium and its alloys.

In bimetallic corrosion under atmospheric conditions, the unhindered transport of oxygen to the surface promotes the passivity of the anode. In the space industry, it is common practice to chemically 'passivate' the materials used to avoid general surface corrosion of the individual subsystems prior to launch.

For the assessment of the corrosion of a bimetallic couple, it is therefore sensible to use the static corrosion potential of the materials in their passive state.

7.2 **Remedies against bimetallic corrosion**

In order to avoid the phenomenon of bimetallic corrosion successfully, one must control the principal factors involved in this type of corrosion, i.e. the presence of an atmosphere and/or the electrical contact between the two materials involved.

Introducing an insulation layer between the two materials is a very effective means of avoiding bimetallic corrosion, but is not always possible in practice, owing to the complexity of spacecraft metal structures and the need for adjacent subsystems to be electrically connected in order to avoid in-orbit charging problems.

Lowering the electrical conductivity of the electrolyte layer on the surface is also an effective remedy. This is achieved by reducing the moisture content or the amount of active gases in the atmosphere. Sometimes extreme steps must be taken, such as almost completely eliminating oxygen from the air (e.g. hermetic sealing of the parts in nitrogen or argon).

The above-mentioned remedies are not always practical in real life, and complete avoidance of bimetallic corrosion can only be achieved if there is a suitable choice of materials involved in the bimetallic couple.

As a general comment on the storage of spacecraft components and subsystems, one can say that it is important to reduce the possibility of bimetallic corrosion both by careful selection of the metal alloy composition and by controlling the surrounding atmosphere.

As a rule of thumb the following guidelines are generally accepted in the space industry: [15,16]

1. A difference in the static corrosion potential of the two metals forming a bimetallic couple of less than 0.5 V is acceptable if the item containing the couple is held in a clean-room atmosphere at all times.
2. If the item containing the bimetallic couple is not held in a clean-room atmosphere, the allowable difference in static corrosion potential must be less than 0.25 V.
3. If it is not possible to follow guidelines 1 and 2, then it will be necessary to provide for an insulation layer or special packaging.

Similar guidelines can be found in Reference 17, where a metals compatibility index chart, based on practical experience, is given for the same metals and alloys as those found in References 15 and 16.

8. Conclusion

A thin condensed film of moisture can be formed on surfaces at relative humidities lower than 100 % . The unhindered transport of oxygen through this film promotes the formation of a 'passivation' layer on the anode material. The polarisation of the anode therefore strongly depends on the relative humidity of the surrounding atmosphere. The low current densities experienced and the surplus of oxygen determine the cathodic process to be the ionisation of oxygen.

Owing to the lack of experimental data in the literature, a simplified procedure for the establishment of the amount of corrosion for bimetallic corrosion couples has to be performed. This simplified procedure is compared with more elaborate calculations and, for eight material combinations, found to be in good agreement. This gives confidence that the amount of corrosion for bimetallic couples under the conditions stated can be estimated with reasonable accuracy for other bimetallic combinations.

References

1. ASTM Subcommittee VIII on Galvanic and Electrolytic Corrosion, ASTM Proc. 39, 247 (1939).
2. ASTM Subcommittee VIII on Galvanic and Electrolytic Corrosion, ASTM Proc. 48, 167 (1948).
3. BS PD 6484:1979, BSI, London, Commentary on Corrosion at Bimetallic Contacts and its Allevation.
4. Kucera V and Mattson E 1982, Atmospheric corrosion of bimetallic structures. *Atmospheric Corrosion,* W H Ailor (Ed.), John Wiley and Sons, Inc., p. 561.
5. Shreir L L 1976, *Corrosion,* Vols. I and II, 2nd ed., Newnes-Butterworth.
6. Tomashov N D 1966, Theory of Corrosion and Protection of Metals, Academy of Sciences, Moscow. ed. B H Tytell, I Geld, H S Preiser, The MacMillan Company.
7. Spedding D J 1977, *Corrosion Science, 17, 173.*
8. Spedding D J 1972, *British Corrosion Journal, 7, 281.*
9. Uhlig H H 1971, *Corrosion and its Control,* 2nd edition, John Wiley and Sons, Inc.
10. Uhlig H H 1947, *Corrosion Handbook,* John Wiley and Sons, Inc.
11. *NACE Corrosion Engineer's Reference Book, 1980,* R S Treseder (Ed.).
12. *Smithells Metals Reference Book,* 6th edition, 1983 A Brandes (Ed.).
13. *Alcoa Aluminium Properties, l-3,* Phys . Diagrams.
14. Mil-std-889b, 1976, *Dissimilar Metals.*
15. ESA-PSS-01-701, *Data for Selection of Space Materials,* November 1985, European Space Agency.
16. MSFC-Spec-250(1), *General Spec. for Protective Finishes for Space Vehicles Structures and Associated Flight Equipment.*
17. Littlefield C F, Groshart E C 1963, *Machine Design, 35, 243.*

Manuscript received 27 July 1989